Cement and Concrete Composites 73 (2016) 203–212

Contents lists available at ScienceDirect

Cement and Concrete Composites

journal homepage: www.elsevier.com/locate/cemconcomp

Coupled effects of crack width, slag content, and conditioning alkalinity on autogenous healing of engineered cementitious composites

Jishen Qiu, Han Siang Tan, En-Hua Yang*

School of Civil and Environmental Engineering, Nanyang Technological University, Singapore 639798, Singapore

ARTICLE INFO

Article history:
Received 9 March 2015
Received in revised form
30 June 2016
Accepted 21 July 2016
Available online 28 July 2016

Keywords:
Engineered cementitious composites
Autogenous healing
Crack width
Slag content
Conditioning alkalinity
Coupled effect

ABSTRACT

Engineered cementitious composite (ECC) is a unique group of fiber-reinforced strain-hardening cementitious composites exhibiting crack self-healing. Due to the absence of coarse aggregates in the ECC mix design, high amount of supplementary cementitious materials (SCM) are generally used to reduce the cement content. The inclusion of slag not only changes the chemical compositionss of the matrix but also alters the crack width of ECC. Both may influence the autogenous healing potential of the slag-based ECC. This paper systematically investigates the influence of the individual factor, i.e. slag content, crack width, and environmental alkalinity, on the autogenous healing efficiency of ECC. Specifically, single-cracked ECC specimens with different slag content and crack width were conditioned under water/dry or NaOH/dry cycles. The autogenous healing performance was evaluated based on crack width reduction, resonant frequency recovery and microstructure analysis. The results show that autogenous healing is determined by a couple effect of physical properties (crack width), chemical compositionss (slag content), and environmental conditions (conditioning alkalinity). At a given slag content and certain alkalinity, there exists a maximum allowable crack width for complete healing, beyond which only partial or no healing would happen. The dominant healing product for the water/dry conditioning is $CaCO_3$ while the NaOH/dry cycles promote slag hydration and results in the formation of C–S–H and $CaCO_3$ as main healing products. It is concluded that $CaCO_3$ precipitation is more effective to engage autogenous healing than the formation of C–S–H. The concept to associate allowable crack width and slag content is proposed, which would guides ingredients selection and component tailoring to engage robust autogenous healing in ECC in the future.

1. Introduction

Infrastructures, for public transportation, energy harvesting, and commercial activities, are vital to the economic well-being of a nation and life quality of the citizens. While the importance of infrastructures in economic development is well recognized, the disrepair, especially of concrete structures, is reaching an alarming level. In most developed countries, concrete maintenance and rehabilitation cost about 50% of the outlay on infrastructures [1]. While the effort in maintenance is undoubtedly important, improving the durability of concrete is the only fundamental solution in the long term.

Deterioration of concrete infrastructure, such as corrosion of reinforcing steel, is associated with the formation of cracks. Reinforced concrete members could crack under structural loading, but more often due to constrained shrinkage/thermal deformations, which are practically inevitable [2]. Cracks in concrete become the pathways for various aggressive agents to penetrate, which accelerates deterioration of reinforced concrete structures; they also reduce the load capacity of some unreinforced concrete members such as plain concrete pavement [3] and concrete railway sleepers [4]. As a result, it is highly desirable to engage self-healing in concrete, i.e. the cracks being healed in natural environment without human interference.

The phenomenon of self-healing in cement-based material has been known for many years. It was observed that cracks of some old concrete structures were lined with white crystalline material, which demonstrated that concrete itself is capable of sealing the

* Corresponding author.
E-mail address: ehyang@ntu.edu.sg (E.-H. Yang).

http://dx.doi.org/10.1016/j.cemconcomp.2016.07.013
0958-9465/

cracks with certain new substance, which were chemically formed in presence of water from the rain and carbon dioxide in the air. A number of studies [5–7] investigated water permeation through cracked concrete, also noted a gradual reduction of permeability over time, which again demonstrated the capability of the cracked concrete to seal itself.

Two approaches have been developed to promote self-healing in concrete. The first approach, referred to as autonomic healing [8], embeds capsules or packets containing self-healing compounds to the concrete matrix [9–13]. In the encapsulation-based approach, the capsules contain chemical compounds, either two-part adhesives or additional matrix resins [14,15]. When the capsules are broken by the propagating crack, the compound is released exclusively into the damaged location, resulting in immediate and efficient repair. Despite the obvious advantage in self-healing efficiency, the amount of required healing compound increases rapidly as crack grows and widens, which causes very high cost [16].

The second approach relies on the self-healing ability of the concrete matrix itself. It is usually referred to as autogenous healing [17]. This approach relies on the homogenous and pervasive distribution of healing compounds, e.g. free calcium ions and unhydrated cement particles in concrete matrix [18,19]. Upon cracking, these compounds are activated by contacting water and carbon dioxide present in the natural environment and form healing products to fill cracks. Such healing products normally take the form of calcite precipitates and/or additional hydration products. Autogenous healing turns the deteriorating environmental agents into beneficial healing reagents. Despite the relatively lower healing efficiency compared to encapsulation-based approach, autogenous healing offers great potential for long-term functionality, and requires relatively lower cost [20,21]. However, lack of reliability is the major obstacle to achieve robust autogenous healing. For instance, while some of the cracks in old concrete structures were healed, more of them remain unhealed [20]. It has been reported that crack width control is essential to form healing products within cracks [5–7]. Finer crack width, which helps to maintain the relatively high alkalinity for calcite precipitation, is more likely to induce autogenous crack healing [5]. Unfortunately, such tight cracks are often difficult to achieve in normal reinforced concrete structures [22].

Engineered cementitious composite (ECC) is a unique group of fiber-reinforced strain-hardening cementitious composites exhibiting ultra-high ductility of several percent with the formation of multiple fine cracks [23–25]. Fig. 1 illustrates the relationship between tensile stress, strain, and average crack width in a typical polyvinyl alcohol (PVA) fiber-reinforced ECC. As can be seen, the crack width increases gradually with the increase of tensile stress and stabilizes at around 60 μm after tensile strain of 1%, i.e. the crack width in ECC is self-controlled and can be regard as an intrinsic property of the material [17]. Autogenous healing are more likely to happen in such tight cracks in PVA-ECC [17,26–28], but the degree of healing of ECC is still highly affected by the crack width. As shown in Fig. 2, Yang et al. [17] found that for the typical PVA-ECC, the smaller cracks are more likely to heal. Specifically, the maximum allowable crack width to obtain complete resonant frequency recovery through autogenous healing was around 50 μm; partial recovery was observed for cracks between 50 and 150 μm; cracks beyond 150 μm did not show any recovery.

Ground granulated blast furnace slag (GGBS) is often used as a supplementary cementitious material (SCM) in concrete [29]. GGBS can be activated in the alkaline environment in concrete, contributing to the compressive strength in a long-term [29,30]. The inclusion of slag changes the autogenous healing efficiency of normal concrete. Van Tittelboom et al. [35] have shown that under

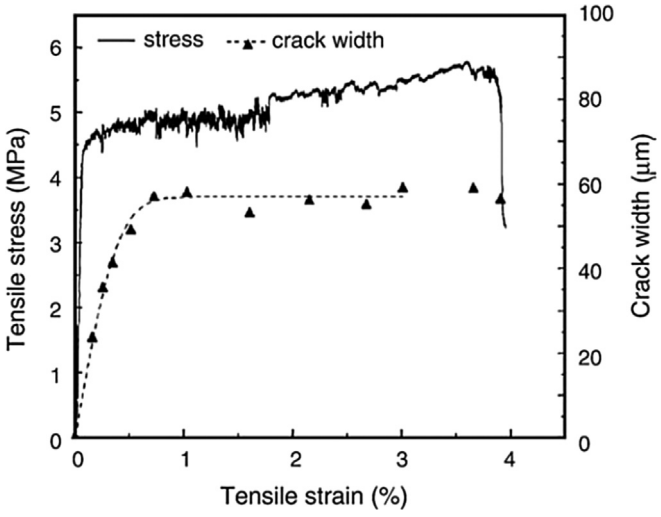

Fig. 1. Typical tensile stress-strain-crack width curve of ECC [17].

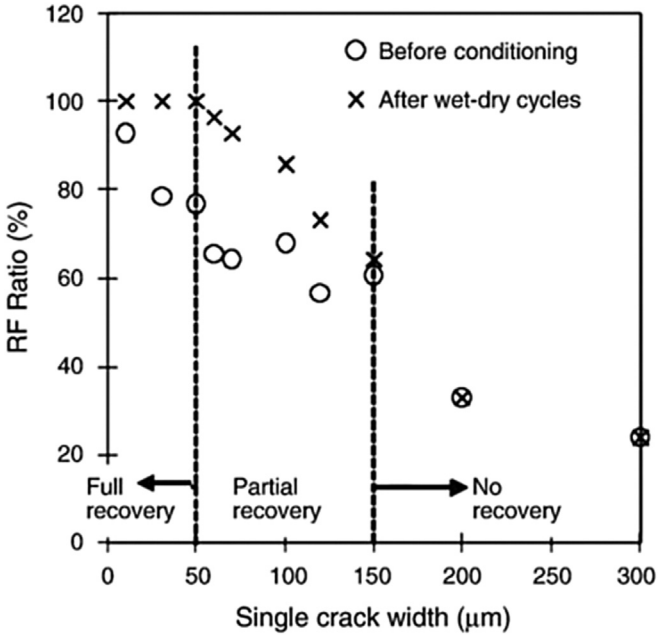

Fig. 2. Resonant frequency (RF) ratio as a function of crack width [17].

continuous water conditioning, replacing cement with blast furnace slag at 50% led to the highest crack closing rate compared to the 0% and 85% replacement. Huang et al. [36] concluded that the blended slag cement paste (66% wt.) had higher autogenous healing potential than Portland cement paste.

In ECC mix design, due to the absence of coarse aggregates, the cement content is much higher than conventional fiber-reinforced concrete. As a result, GGBS is often suggested as cement replacement in ECC mix design [31–34]. Qian et al. [32] studied the self-healing behavior of ECC adopting high slag content and concluded that the healing efficiency was comparable with that of ECC that has zero slag. Sahmaran et al. [37] found that in slag-rich ECC, cracks up to 100 μm were completely sealed after 60 days of continuous water conditioning. All results reported in the previous studies; however, were the combined effects from changes of chemical compositionss of matrix and crack width of composite due to the addition of slag. All study failed to separate the

influences of the two potential sources, i.e. chemical compositionss and crack width, on the autogenous healing behavior of slag-based ECC. No systematic study has been carried out in this regard. In addition, the effect of high alkalinity on the autogenous healing of slag-based ECC is rarely studied.

The inclusion of slag not only changes the chemical compositionss of the matrix but also alters the crack width of ECC [33,34]. Both may influence the autogenous healing potential of the slag-based ECC, which is determined by a coupled effect of physical properties (crack width), chemical compositions (slag content), and very likely environmental conditions (alkalinity). It is therefore necessary to understand the contribution from individual factor on the autogenous healing behavior. This form the basis to have a complete understanding of the coupled effects of crack width, slag content, and environmental alkalinity on the autogenous healing behavior o slag-based ECC, which represent the bottleneck to predict and to design slag-based ECC with robust autogenous healing.

This paper systematically investigates the influence of the individual factor, i.e. slag content, crack width, and environmental alkalinity, on the autogenous healing efficiency of ECC. The degree of healing was evaluated through the measurement of crack width reduction and resonant frequency recovery. Microstructure analysis was engaged to reveal the chemical compositions of the healing products. The feasibility of quantifying the coupled effect and predicting the autogenous healing behavior of slag-based ECC is discussed.

2. Experimental program

ECC specimens with different slag content were prepared. The specimens were pre-loaded to form a single crack with pre-determined crack width up to 300 μm, followed by conditioning the pre-cracked specimens in different environmental conditions. The autogenous healing performance was evaluated based on crack width reduction, resonant frequency recovery, and microstructure analysis. The detailed experimental program is given in the following sections.

2.1. ECC specimen preparation

Type I Portland cement (CEM I 52.5 N), GGBS, fine aggregates, and polyvinyl-alcohol (PVA) fibers, superplasticizer (SP) and tap water were used as ingredients for ECC specimen preparation. The GGBS (particle size less than 100 μm) was produced by quenching and drying the molten iron slag from normal blast-furnace. The elementary composition of GGBS is shown in Table 1. The fine aggregates (particle size less than 600 μm) were obtained by sieving normal river sand. The PVA fibers are of 12 mm in length, 39 μm in diameter, and have a nominal tensile strength of 1600 MPa.

Three levels of slag content, i.e. 0%, 30%, and 60% cement replacement, were studied as shown in Table 2. The water-to-binder (cement and GGBS) ratio was fixed at 0.30, while the GGBS-to-binder ratio ranged from 0% to 60%. Since the crack width in ECC is self-controlled, lower fiber dosage was adopted in Mixes 4 to 6 in order to obtain crack width larger than 100 μm.

Table 1
Elementary composition of GGBS.

CaO	39.43%
SiO_2	31.19%
Al_2O_3	13.41%
MgO	9.32%
SO_3	4.25%
Others	2.40%

Cement, GGBS, and fine aggregates were dry mixed first with a three-gear planetary mixer for two minutes. Water and SP were slowly added to the mixture at low mixing speed within one minute, followed by medium mixing speed for another two minutes to achieve the required rheology of the fresh mortar. PVA fibers were then slowly added into the mixture at low mixing speed within one minute, followed by medium mixing speed for three minutes to ensure good fiber dispersion.

The fresh mixture was cast into molds of dog-bone specimens (Fig. 3a) for uniaxial tensile testing (Fig. 3b) and self-healing tests, and cube specimens ($50 \times 50 \times 50$ mm^3) for compressive tests. The specimens were de-molded after one day and were cured in laboratory air (20 °C, 80%RH) until the pre-determined age. Uniaxial compressive and tensile tests were conducted for ECC specimens at the age of 28 days. At least three specimens were tested and the mechanical testing results are given in Table 3.

2.2. Self-healing tests

2.2.1. Pre-cracking

At the age of 40 days, dog-bone specimens were pre-cracked using the same set-up (Fig. 3b) as used for the uniaxial tensile test. A single crack with pre-determined crack width up to 300 μm was introduced in each specimen by controlling the pre-cracking load level. At 2% fiber content, i.e. GGBS0 to 60, the crack width of ECC is self-controlled and it would not be possible to extend crack widths beyond 100 μm without generating a second crack. As an alternative, GGBS0a to 60a with lower fiber content were used to produce larger single crack up to 300 μm. After pre-cracking, the load was released and the crack width was measured with optical microscope, the details of which are given in the section on crack width measurement.

2.2.2. Self-healing conditioning regime

Two different wet/dry cycles were used as conditioning regimes to engage autogenous healing. The first type of wet/dry cycle consisted of submerging the specimens in water (20 °C) for one day, followed by exposing the specimens to air (20 °C, 80%RH) for another day, which was suggested by Yang et al. [17]. The second type of wet/dry cycle consisted of one day in NaOH solution (pH = 13, 20 °C) followed by another day in air (20 °C, 80%RH). The later conditioning regime was used to encourage slag hydration through alkali activation. For each slag content and each type of wet/dry cycle, three uncracked virgin specimens were also conditioned for 14 wet/dry cycles as control.

2.2.3. Crack width measurement

Crack width reduction on both sides of the specimen surface was measured as a direct assessment of self-healing. The crack width was measured at a specific location, i.e. the same location, before and after conditioning on the specimen surface. At least three locations were measured for each specimen. At least six specimens were used to obtain crack width reduction for each combination of slag content and conditioning alkalinity. Images of all pre-cracked specimens before and after conditioning were taken at magnification of 210 × by Nikon DS-Fi2 high resolution camera. The high-magnification images were used to monitor changes of crack width.

2.2.4. Resonant frequency measurement

Resonant frequency (RF) can be used to determine the stiffness and to characterize damage in concrete. In this study, recovery of transverse resonant frequency (TRF) of single-cracked dog-bone ECC specimen was adopted to characterize the stiffness recovery as

Table 2
Proportions of mix design in current research.

Mix. no	Cement (kg/m^3)	GGBS (kg/m^3)	Sand (kg/m^3)	Water (kg/m^3)	PVA fiber (kg/m^3)	SP (L/m^3)	Cement replacing ratio	w/b ratio
1 (GGBS0)	1411	0	282	423	26[a]	3.6	0.00	0.30
2 (GGBS30)	976	418	279	418	26[a]	3.0	0.30	0.30
3 (GGBS60)	551	827	276	414	26[a]	2.4	0.60	0.30
4 (GGBS0a)	1411	0	282	423	8.5[b]	3.6	0.00	0.30
5 (GGBS30a)	976	418	279	418	8.5[b]	3.0	0.30	0.30
6 (GGBS60a)	551	827	276	414	8.5[b]	2.4	0.60	0.30

[a] The fiber content was fixed at 2% in volume fraction.
[b] The fiber content was fixed at 0.65% in volume fraction.

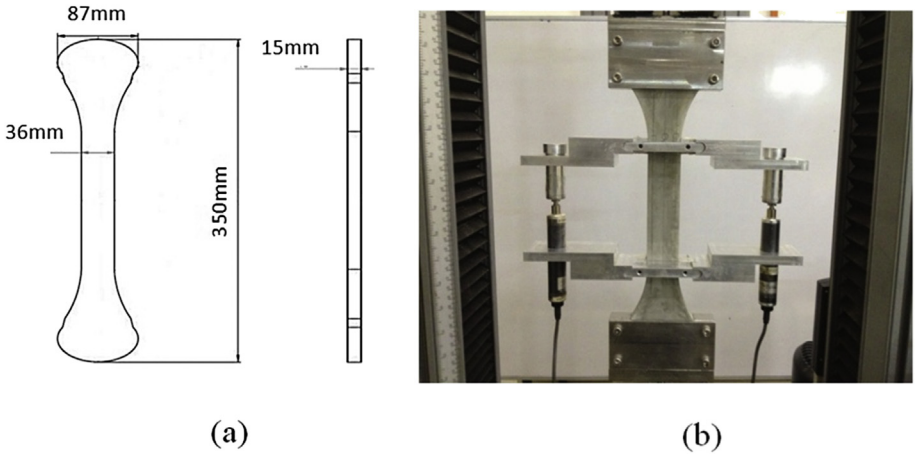

Fig. 3. Illustration of (a) dog-bone specimen dimensions and (b) uniaxial tensile test set-up (x ton UTM, loading rate 0.04 mm/min).

Table 3
Mechanical properties of ECC.

	Compressive strength (MPa)	Tensile strength (MPa)	Tensile ductility (%)
GGBS0	63.1 ± 3.8	4.25 ± 0.48	1.12 ± 0.36
GGBS30	66.3 ± 3.7	4.40 ± 0.19	1.05 ± 0.07
GGBS60	70.8 ± 1.8	4.88 ± 0.62	1.26 ± 0.28

an indicator of autogenous healing, as similar method was used by Yang et al. [17].

TRF of all specimens was measured before healing conditioning and before the beginning of every conditioning cycle when the specimens were dry. Specifically, the TRF measurement adopted the impact method suggested by ASTM C215 (Standard Test Method for Fundamental Transverse, Longitudinal, and Torsional Resonant Frequency of Concrete Specimens). In this method, the dog-bone specimen was placed on two roller supports that are 200 mm to each other; a small hammer was used to vertically strike the specimen at its end; the vibration was determined with a sensor placed on the center of the specimen so that the TRF could be determined with the help of a resonant frequency meter (Controls 58-E0035/C).

The normalized TRF, i.e. the ratio of TRF of pre-cracked specimen to TRF of uncracked specimens (average of three) with the same conditioning regime, was calculated and reported. For each combination of slag content and conditioning alkalinity, the TRF of at least seven specimens (crack width distributed from 0 to 300 μm) were tested and their normalized TRF were calculated. Uncracked specimens were included as control group for normalization because TRF also increased after conditioning due to further hydration of the matrix, the effect of which must be excluded from true healing-induced TRF recovery.

2.2.5. SEM/EDX

Characterization of the healing products was carried out in addition to the crack width and TRF measurement. After conditioning, the morphology of healing products in the cracks was observed with field emission scanning electron microscopy (FE-SEM, JSM-7600F). Energy-dispersive X-ray spectroscopy (EDX, Oxford X-Max 80 mm^2) was used to determine the chemical compositions of the healing products. All the SEM/EDX samples were obtained from the internal part of the specimen, about 7 mm from the specimen surface.

3. Results and discussion

3.1. Crack width reduction

It was observed that crack width reduced with conditioning cycles as crystal-like substances grew in the crack. In the current study, the crack width reduction in pre-cracked ECC specimens is measured and used as a direct assessment of autogenous healing at different slag content under conditioning regime.

Figs. 4 and 5 show the surface crack width of GGBS0, GGBS0a, GGBS30, GGBS30a, GGBS60, and GGBS60a specimens before and after 14 water/dry and NaOH/dry conditioning cycles, respectively. A 45-degree reference line representing zero-healing (blue dashed line) was plotted. Data points below the reference line indicate reduced crack width after healing. A linear trend line (red solid line) was plotted to fit these data points. As can be seen, for all the three groups, surface crack width was reduced under water/dry or NaOH/dry conditioning cycles. While crack width reduction on the surface was measured in all specimens with crack width up to around 300 μm, only very fine cracks (<30 μm) could possibly be completely sealed.

The crack width reduction ratio, as defined by Equation (1), was

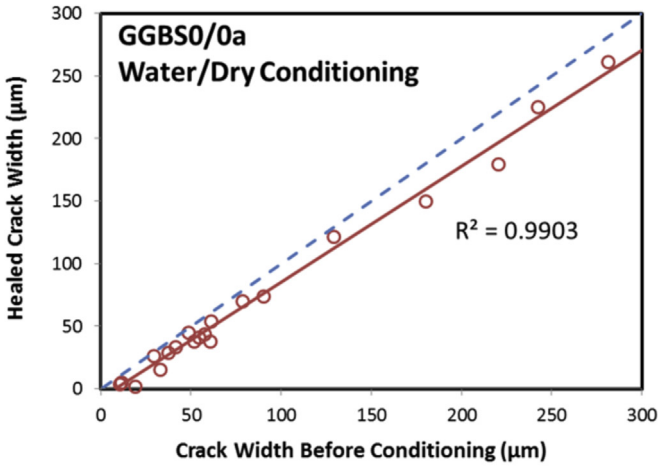

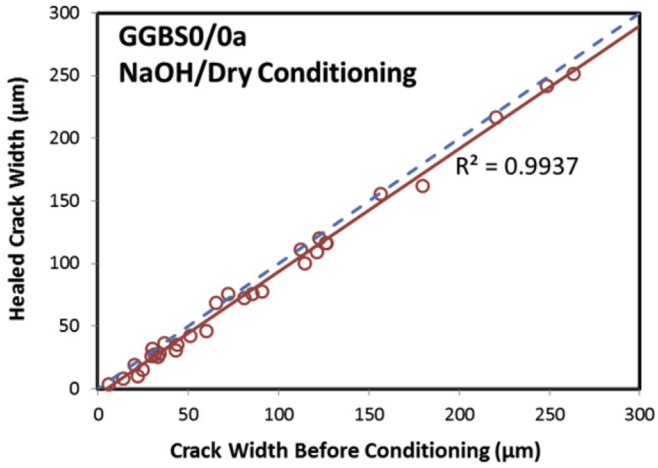

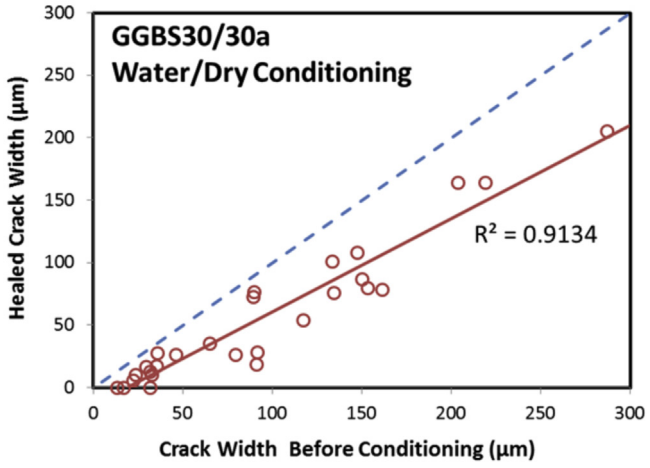

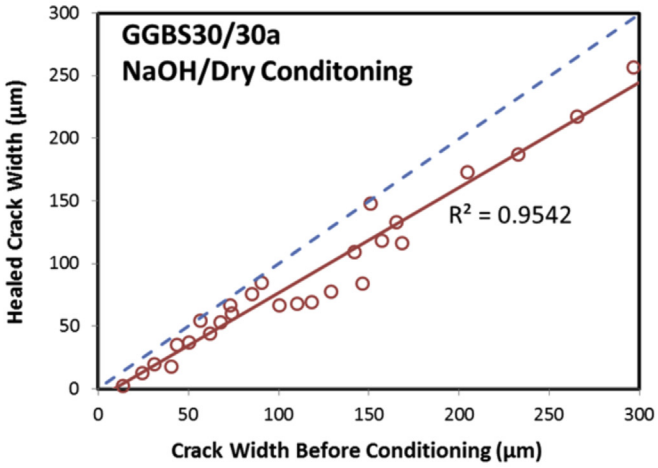

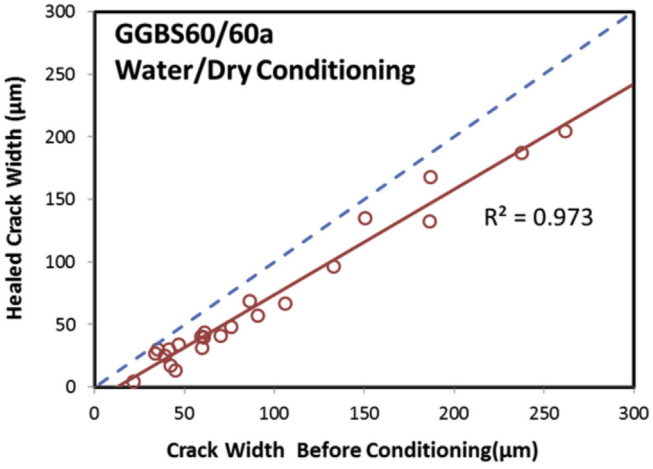

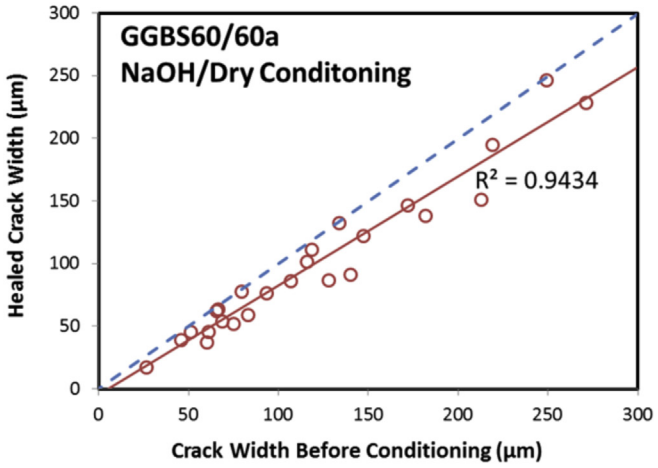

Fig. 4. Crack width of pre-cracked GGBS0/0a, GGBS30/30a, and GGBS60/60a ECC specimens before and after 14 water/dry conditioning cycles, each point stands for one crack width measurement location.

Fig. 5. Crack width of pre-cracked GGBS0/0a, GGBS30/30a, and GGBS60/60a ECC specimens before and after 14 NaOH/dry conditioning cycles, each point stands for one crack width measurement location.

calculated for each measured location. In Equation (1), w_0 and w represent the crack width before and after conditioning, respectively.

$$\textit{Crack width reduction ratio}(\%) = (w_0 - w)/w_0 \quad (1)$$

Fig. 6 plots a typical relationship between the crack width reduction ratio and the original crack width. As can be seen, smaller cracks show higher efficiency on the crack width reduction. To quantitatively compare the degree of healing of different ECC groups (GGBS0, 30, and 60) and under different conditioning regimes (water/dry and NaOH/dry cycles), the crack width reduction ratio at original crack width of 50, 100, and 200 μm were

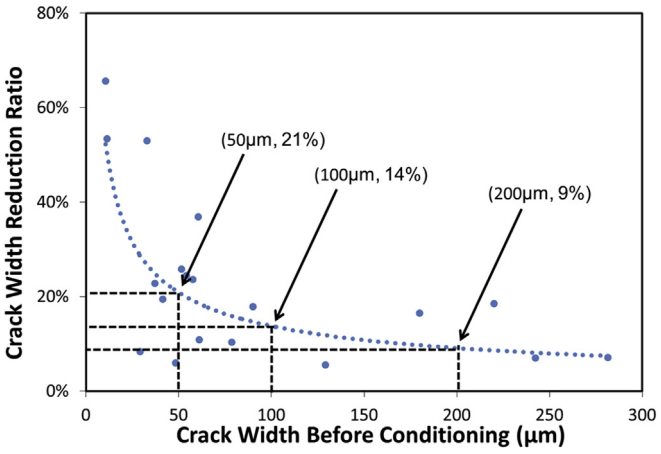

Fig. 6. Typical relationship between the crack with reduction ratio and the original crack width and illustration of determining the crack width reduction ratio at certain original crack width. The data points were obtained from GGBS0 under water/dry conditioning cycles, original crack width of 50, 100, 200 μm were selected for current study.

determined with a fitted curve as shown in Fig. 6. Fig. 7 shows the crack width reduction ratio of ECC with different slag content and under different environmental alkalinity. As can be seen, slag content greatly affected the reduction of crack width for both conditioning regimes. Specifically, GGBS0 showed the least crack width reduction while GGBS30 exhibited the highest potential to engage autogenous healing. ECC specimens exposed to the water/dry conditioning regime showed more pronounced crack width reduction as compared to the NaOH/dry conditioning regime.

3.2. Resonant frequency recovery

Figs. 8 and 9 show the normalized TRF of pre-cracked ECC specimens before (blue cross) and after (red circle) 14 water/dry or NaOH/dry conditioning cycles, respectively. As can be seen, pre-cracking greatly reduced resonant frequency of ECC specimens (blue cross) and the reduction increased with increasing crack width, indicating more damage. After conditioning, the resonant frequency recovered and in some cases even to its original level. In this study, because of the variation of specimen quality, normalized TRF recovery to 97% was accounted as complete recovery.

As can be seen in Fig. 8, GGBS30 showed the highest potential to obtain healing in terms of TRF recovery as compared to GGBS0 and GGBS60. It was observed that under water/dry conditioning environment, GGBS30 allowed complete recovery of TRF as long as the crack width is less than around 90 μm while the maximum allowable crack width for GGBS60 and GGBS0 were around 60 μm and 40 μm, respectively. In Fig. 9, under NaOH/dry conditioning, GGBS30 again showed the most significant TRF recovery with a

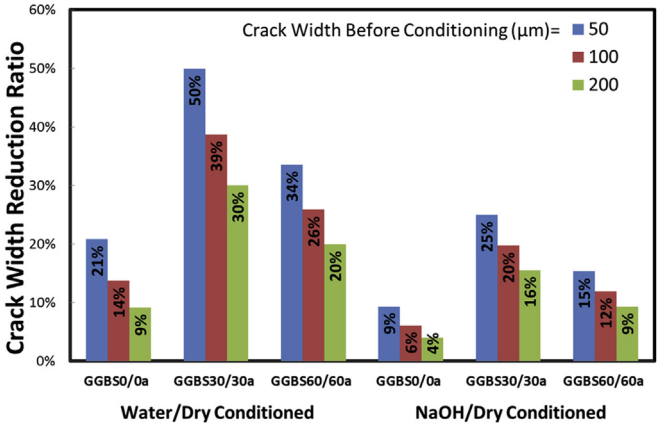

Fig. 7. The effect of original crack width, slag content, and conditioning alkalinity on the crack width reduction ratio determined from Fig. 6.

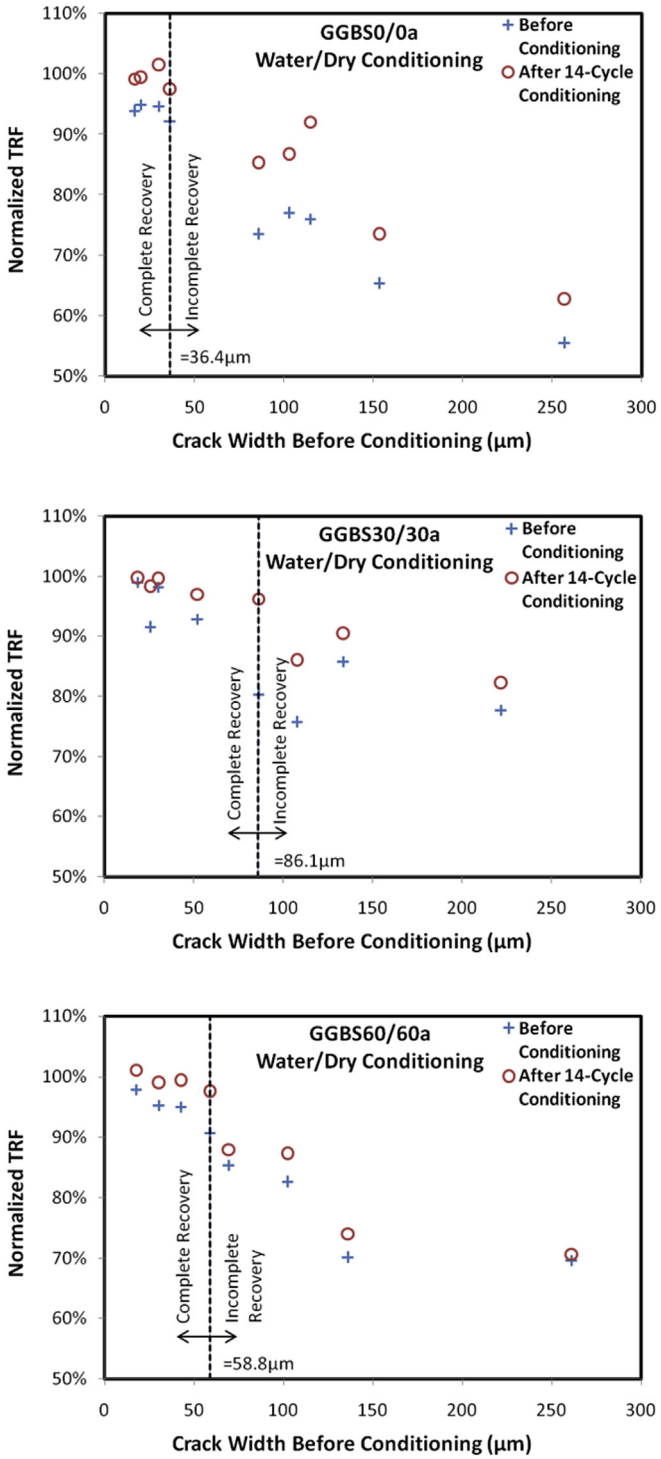

Fig. 8. Normalized transverse resonant frequency (TRF) as a function of crack width before and after 14 water/dry conditioning cycles; each pair of cross and dot stands for one specimen, the crack width was determined by taking the average of all the measured locations.

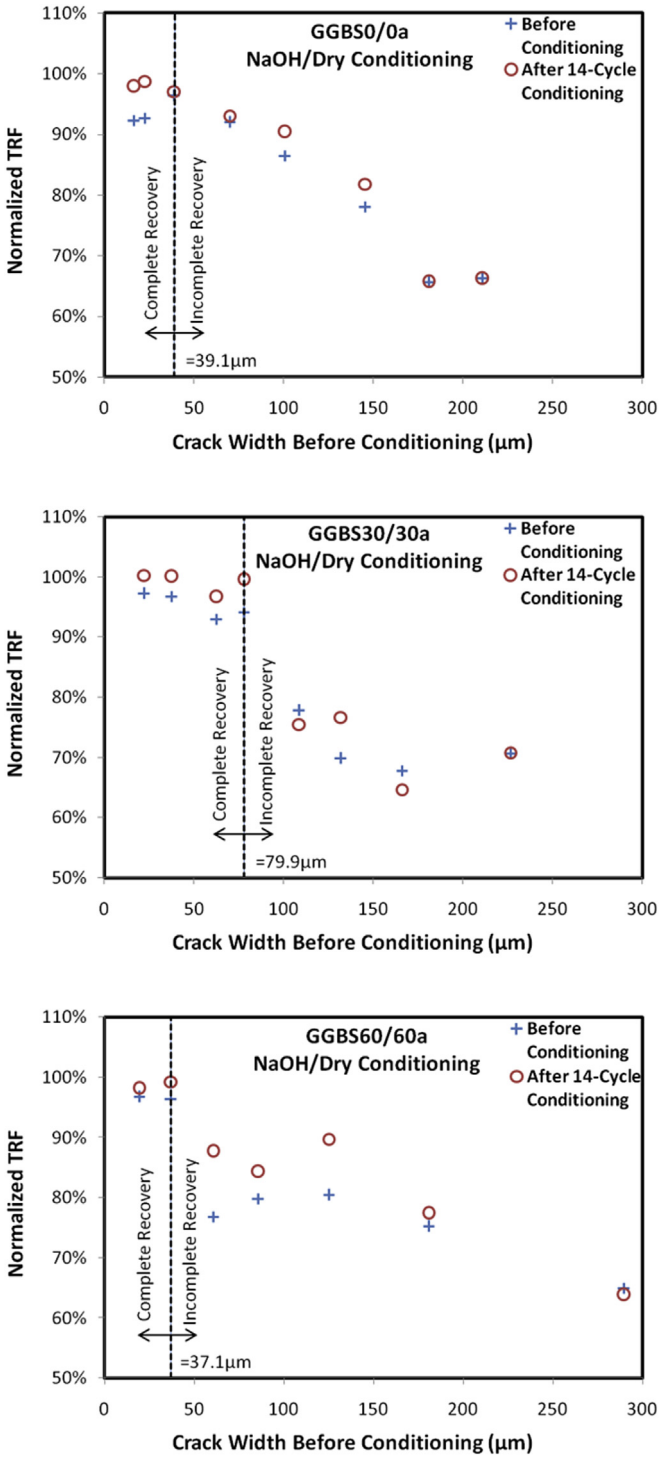

Fig. 9. Normalized transverse resonant frequency (TRF) as a function of crack width before and after 14 NaOH/dry conditioning cycles; each pair of cross and dot stands for one specimen, the crack width was determined by taking the average of all the measured locations.

maximum allowable crack width around 80 μm while that for GGBS60 and GGBS0 were both around 40 μm.

The relationship between normalized TRF recovery and crack width reduction ratio was plotted in Fig. 10 to understand the mechanical recovery of partially healed specimens. In Fig. 10, each data point was obtained with one specimen and the specimens with complete TRF recovery were not included. A trend can be seen

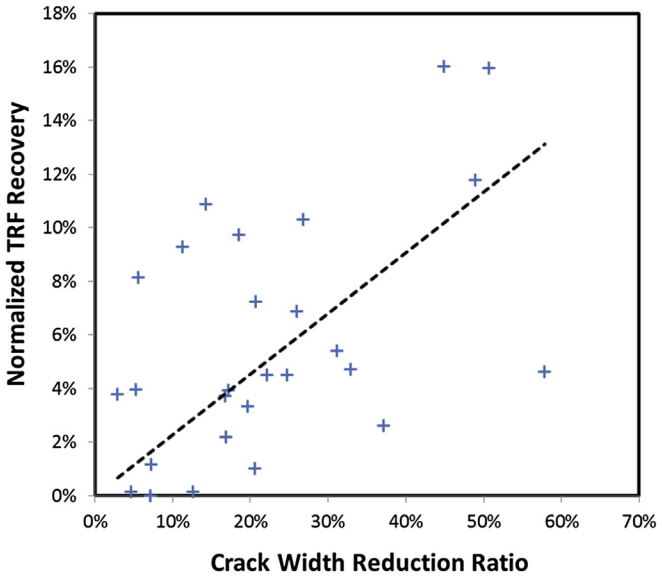

Fig. 10. Positive correlation between the normalized TRF recovery and the crack width reduction ratio.

that the TRF recovery increases with the crack width reduction ratio. This suggests the two evaluation methods have certain positive correlation.

3.3. SEM and EDX

Fig. 11a shows the SEM image of a healed crack and Fig. 11b and c illustrates the typical morphology of the healing products. It can be seen that healing products, distinct from the matrix, grew in the crack and almost fill the 100 μm gap. The healing products are composed of irregularly precipitated crystal-like particles. While the large particles (≥10 μm, Fig. 11a) fill the major portion of the gap, smaller particles (≤10 μm, Fig. 11b) can be found in the void between the large particles and crack surface. In Fig. 11c it is seen that the crystal-like particles grow from very small precipitates, several hundreds of nanometers in size. It is also observed that healing products precipitate on the PVA fiber as shown in Fig. 12. Fiber bridging might very likely facilitate the precipitation of healing products and promotes healing in ECC [38].

The chemical compositions of the healing products were determined with EDX for ECC samples at different slag content for different conditioning regimes. At least three locations were analyzed for each group and the average values are reported in Table 4. As can be seen, the healing products are mainly composed of calcium, silicon, and carbon which suggests the presence of $CaCO_3$ and/or C–S–H as the main healing products as reported in many other studies [17,32,38,39]. A much lower Ca/Si ratio (1.21–3.81) of the healing products was observed for samples subjected to the NaOH/dry cycles. It is known that the Ca/Si ratio of C–S–H is around 2.0 [36,40]. This indicates that a mixture of C–S–H from continued hydration and $CaCO_3$ from carbonation is the major healing products in samples subjected to the NaOH/dry cycles. The Ca/Si ratio of the healing products for the samples subjected to the water/dry cycles; however, is much higher in the range of 5.63–7.18. This suggests that $CaCO_3$ from carbonation are the dominant healing product in samples subjected to water/dry cycles.

3.4. Discussion

Preceding sections show that slag content greatly affects the

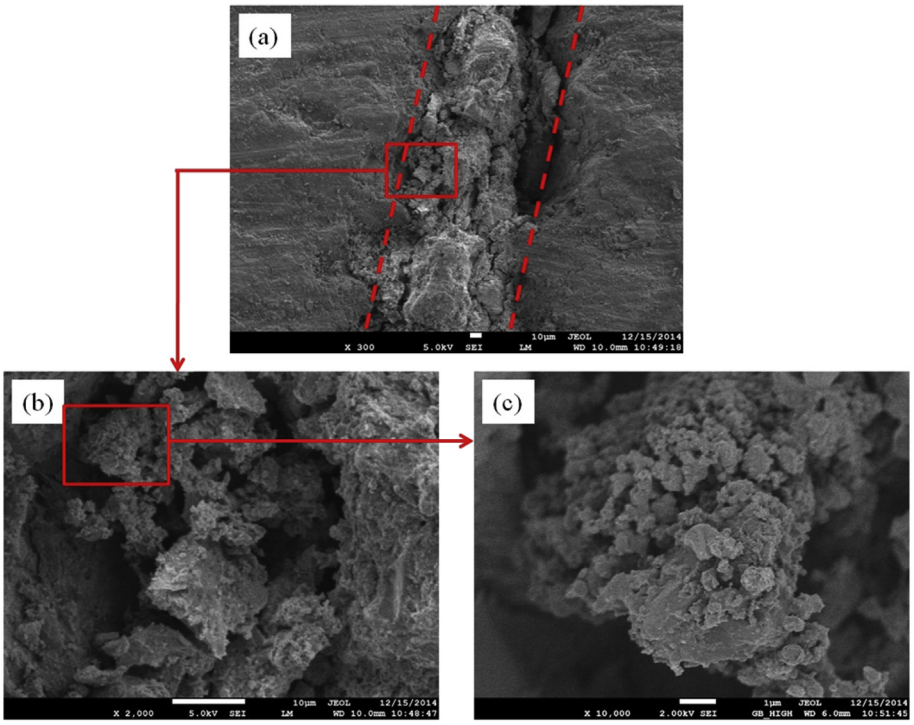

Fig. 11. (a) A healed crack in GGBS30 specimen subjected to 14 water/dry conditioning cycles; (b) and (c) Typical morphology of the healing products at 2000 × and 10,000 × magnification, respectively.

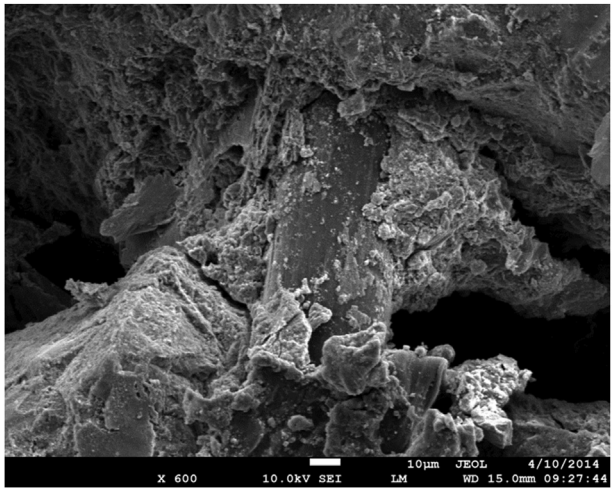

Fig. 12. Self-healing products precipitated on PVA fiber.

autogenous healing of ECC. Compared with GGBS0 and GGBS60, GGBS30 exhibits the most crack width reduction (Fig. 6) and resonant frequency recovery (Figs. 8 and 9). The precipitation of $CaCO_3$ highly depends on the amount of free Ca^{2+} ions leached out from the matrix in the wet conditioning. Leachability of calcium ion is related to the concentration of the Ca^{2+} ions in the pore solution in matrix, where $Ca(OH)_2$ is dissolved [30]. The concentration of Ca^{2+} ions in the pore solution depends on two important factors: 1) the amount of $Ca(OH)_2$ available in matrix and 2) the alkalinity of the pore solution. Previous study on hydration of slag-blended cement indicated that replacing cement with slag consumes $Ca(OH)_2$ and lowers the pH of the pore solution [30]. While GGBS30 may have a lower $Ca(OH)_2$ content in the matrix compared to GGBS0, the lower pH in the pore solution of GGBS30 greatly promotes the dissolution of $Ca(OH)_2$ [41], resulting in higher overall free Ca^{2+} concentration in the pore solution of GGBS30. At higher GGBS content, i.e. GGBS60, less $Ca(OH)_2$ is produced from cement hydration and most of the $Ca(OH)_2$ is consumed by slag [42]. Therefore, less free Ca^{2+} is available in the pore solution of GGBS60 compared with GGBS30.

As discussed above, $CaCO_3$ is the dominant healing product for samples subjected to the water/dry cycle while a mixture of $CaCO_3$ and C–S–H represents the major healing products for samples subjected to the NaOH/dry cycle. NaOH/dry conditioning indeed promotes slag hydration as more C–S–H was identified in the

Table 4
Elementary compositions (by mass) of self-healing products.

Element	Water/dry cycle			NaOH/dry cycle		
	GGBS0/0a	GGBS30/30a	GGBS60/60a	GGBS0/0a	GGBS30/30a	GGBS60/60a
Calcium	21.19%	36.67%	34.48%	26.29%	20.24%	18.97%
Silicon	3.41%	5.64%	6.06%	7.09%	8.59%	18.13%
Carbon	14.10%	14.80%	9.84%	10.15%	14.88%	7.52%
Oxygen	55.05%	39.01%	45.81%	45.79%	46.99%	48.96%
Others	6.26%	3.89%	3.81%	10.68%	9.30%	6.42%
Ca/Si	7.18	6.45	5.63	3.81	2.39	1.21

healing products as shown in Table 4. However, the general observation concluded that specimens subjected to the water/dry cycles show more pronounced healing than specimens subjected to the NaOH/dry cycles. This implies that NaOH/dry conditioning regime, while encouraging slag hydration, may suppress the formation of $CaCO_3$ precipitates in cracks as healing products. This may be attributed to the fact that the insolubility of $CaCO_3$ peaks at pH of 9.8 [5] and therefore the increased alkalinity under NaOH conditioning (pH = 13) suppresses $CaCO_3$ precipitation in cracks. Based on the results on crack width reduction (Fig. 6), autogenous healing through $CaCO_3$ precipitation by carbonation (specimens subjected to water/dry cycles) is more effective than that through the formation of C–S–H by alkali-activated slag hydration (specimens subjected to NaOH/dry cycles) in slag-based ECC.

As pointed out in the introduction, the autogenous healing of ECC is governed by a coupled effect of physical properties, chemical compositions, and environmental conditions. In current study, the experimental results quantified TRF recovery through a wide range of crack width for different slag contents, which decoupled the effects of physical properties (crack width) from the chemical compositions (slag content). Such decoupled effects are illustrated in Fig. 13, which shows the maximum allowable crack width to engage complete healing at different slag content. Based on the current results with water/dry conditioning cycles and the result from Qian et al. [32] where ECC experienced similar water/dry cycles, a fitted line was drawn to illustrate this coupled effect of crack width and slag content on the autogenous healing of ECC. The fitted envelope can be used to predict the healing efficiency of slag-based ECC under water/dry conditioning, i.e. at given slag content, if the crack width, either from mechanical loading or restrained shrinkage, is under the envelope, complete autogenous healing is expected, otherwise only partial or even no healing would happen.

Previous studies have shown that the mechanical performance of ECC is highly tailorable and the crack width can be predicted with a micromechanics-based model [43]. As a result, the concept in Fig. 13, i.e. predicting the healing efficiency with physical properties (crack width) and chemical compositions (slag content), can be extended to a practical design chart if more data points are added to form an envelope with higher reliability. In a complete design chart, different envelopes will be drawn for different environmental conditionings.

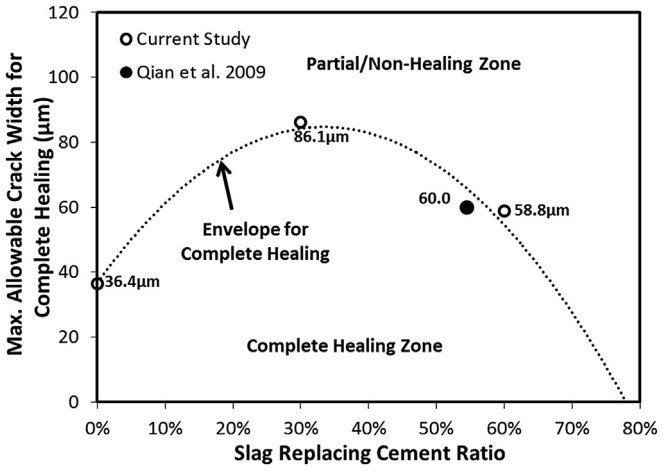

Fig. 13. Autogenous healing of slag-based ECC as a function of crack width and slag content. The data points were drawn based on the current results with water/dry cycles and Qian et al.'s work [32], where ECC experienced similar water/dry cycles.

4. Conclusions

This paper studied the effects of slag content, crack width, and conditioning alkalinity on the autogenous healing behavior of slag-based ECC. Single-cracked ECC specimens with three different slag contents (cement replacement ratio at 0%, 30%, and 60%) and crack width up to 300 μm were conditioned under water/dry or NaOH(pH = 13)/dry cycles. The healing performance was evaluated based on crack width reduction, resonant frequency recovery, and SEM/EDX analysis. Following conclusions can be made in current study.

- ECC autogenous healing is determined by a coupled effect of physical properties (crack width), chemical compositions (slag content), and environmental conditions (conditioning alkalinity). At a given slag content and certain alkalinity, there exists a maximum allowable crack width for complete healing, beyond which only partial or no healing would happen.
- The addition of slag up to 30% enables complete healing of larger crack (86 μm and 80 μm for water/dry and NaOH/dry conditioning cycles). After that, the maximum allowable crack width to engage complete healing reduces with slag content. Water/dray cycles caused more crack width reduction compared to NaOH/dry cycles. Optimum slag addition, smaller crack width and water/dry conditioning cycle favor self-healing in ECC.
- $CaCO_3$ is the dominant healing products for samples subjected to the water/dry cycle while a mixture of $CaCO_3$ and C–S–H represents the major healing products for samples subjected to the NaOH/dry cycle.
- NaOH/dry conditioning promotes slag hydration but suppresses the formation of $CaCO_3$ precipitates in cracks as healing products. $CaCO_3$ precipitation through carbonation is a more effective mean to engage self-healing than the formation of C–S–H through alkali-activated slag hydration.
- In the future, a complete design chart for ECC autogenous healing should consider the coupled effect completely, i.e. including the effect of physical properties, chemical compositions, and environmental conditions, as the concept illustrated in this paper.

Acknowledgements

The authors would like to acknowledge the Ministry of Education, Singapore for the financial support of this research (Project No. RG115/14).

References

[1] V.C. Li, High performance fiber reinforced cementitious composites as durable material for concrete structure repair, Int. J. Restor. 10 (2) (2004) 163–180.
[2] F. Wittmann, Crack formation and fracture energy of normal and high strength concrete, Sadhana 27 (4) (2002) 413–423.
[3] T.F. Fwa, The Handbook of Highway Engineering, CRC Press, 2005.
[4] W. Ferdous, A. Manalo, Failures of mainline railway sleepers and suggested remedies–review of current practice, Eng. Fail. Anal. 44 (2014) 17–35.
[5] C. Edvardsen, Water permeability and autogenous healing of cracks in concrete, ACI Mater. J. Am. Concr. Inst. 96 (4) (1999) 448–454.
[6] H.-W. Reinhardt, M. Jooss, Permeability and self-healing of cracked concrete as a function of temperature and crack width, Cem. Concr. Res. 33 (7) (2003) 981–985.
[7] K. Wang, D.C. Jansen, S.P. Shah, A.F. Karr, Permeability study of cracked concrete, Cem. Concr. Res. 27 (3) (1997) 381–393.
[8] C. Joseph, A. Jefferson, B. Isaacs, R. Lark, D. Gardner, Experimental investigation of adhesive-based self-healing of cementitious materials, Mag. Concr. Res. 62 (11) (2010) 831–843.
[9] C. Dry, Matrix cracking repair and filling using active and passive modes for smart timed release of chemicals from fibers into cement matrices, Smart Mater. Struct. 3 (2) (1994) 118.
[10] C. Dry, Procedures developed for self-repair of polymer matrix composite materials, Compos. Struct. 35 (3) (1996) 263–269.

[11] C. Dry, Release of smart chemicals for the in-service repair of bridges and roadways, in: Proceedings of the Symposium on Smart Materials, Structures and MEMS, 1996.
[12] V.C. Li, Y.M. Lim, Y.-W. Chan, Feasibility study of a passive smart self-healing cementitious composite, Compos. Part B Eng. 29 (6) (1998) 819–827.
[13] J.Y. Lee, G.A. Buxton, A.C. Balazs, Using nanoparticles to create self-healing composites, J. Chem. Phys. 121 (11) (2004) 5531–5540.
[14] S.R. White, N. Sottos, P. Geubelle, J. Moore, M.R. Kessler, S. Sriram, et al., Autonomic healing of polymer composites, Nature 409 (6822) (2001) 794–797.
[15] M. Kessler, N. Sottos, S. White, Self-healing structural composite materials, Compos. Part A Appl. Sci. Manuf. 34 (8) (2003) 743–753.
[16] K. Van Tittelboom, N. De Belie, Self-healing in cementitious materials—A review, Materials 6 (6) (2013) 2182–2217.
[17] Y. Yang, M.D. Lepech, E.-H. Yang, V.C. Li, Autogenous healing of engineered cementitious composites under wet–dry cycles, Cem. Concr. Res. 39 (5) (2009) 382–390.
[18] C. Clear, The Effects of Autogenous Healing upon the Leakage of Water through Cracks in Concrete, 1985.
[19] J. Cowie, F. Glasser, The reaction between cement and natural waters containing dissolved carbon dioxide, Adv. Cem. Res. 4 (15) (1992) 119–134.
[20] M. Wu, B. Johannesson, M. Geiker, A review: self-healing in cementitious materials and engineered cementitious composite as a self-healing material, Constr. Build. Mater. 28 (1) (2012) 571–583.
[21] V.C. Li, E. Herbert, Robust self-healing concrete for sustainable infrastructure, J. Adv. Concr. Technol. 10 (6) (2012) 207–218.
[22] T. Vidal, A. Castel, R. Francois, Analyzing crack width to predict corrosion in reinforced concrete, Cem. Concr. Res. 34 (1) (2004) 165–174.
[23] V.C. Li, S. Wang, C. Wu, Tensile strain-hardening behavior of polyvinyl alcohol engineered cementitious composite (PVA-ECC), ACI Mater. J. 98 (6) (2001) 483–492.
[24] E.-H. Yang, Y. Yang, V.C. Li, Use of high volumes of fly ash to improve ECC mechanical properties and material greenness, ACI Mater. J. 104 (6) (2007) 620–628.
[25] S. Wang, V.C. Li, Engineered cementitious composites with high-volume fly ash, ACI Mater. J. 104 (3) (2007) 233–241.
[26] M. Şahmaran, V.C. Li, Durability of mechanically loaded engineered cementitious composites under highly alkaline environments, Cem. Concr. Compos. 30 (2) (2008) 72–81.
[27] M. Li, V.C. Li, Cracking and healing of engineered cementitious composites under chloride environment, ACI Mater. J. 108 (3) (2011) 333–340.
[28] Y. Zhu, Y. Yang, Y. Yao, Autogenous self-healing of engineered cementitious composites under freeze–thaw cycles, Constr. Build. Mater. 34 (2012) 522–530.
[29] A.M. Neville, Properties of Concrete, 2011.
[30] W. Chen, Hydration of Slag Cement: Theory, Modeling and Application, University of Twente, 2006.
[31] J.-K. Kim, J.-S. Kim, G.J. Ha, Y.Y. Kim, Tensile and fiber dispersion performance of ECC (engineered cementitious composites) produced with ground granulated blast furnace slag, Cem. Concr. Res. 37 (7) (2007) 1096–1105.
[32] S. Qian, J. Zhou, M. De Rooij, E. Schlangen, G. Ye, K. Van Breugel, Self-healing behavior of strain hardening cementitious composites incorporating local waste materials, Cem. Concr. Compos. 31 (9) (2009) 613–621.
[33] J. Zhou, S. Qian, M.G.S. Beltran, G. Ye, K. van Breugel, V.C. Li, Development of engineered cementitious composites with limestone powder and blast furnace slag, Mater. Struct. 43 (6) (2010) 803–814.
[34] Z. Chen, Y. Yang, Y. Yao, Quasi-static and dynamic compressive mechanical properties of engineered cementitious composite incorporating ground granulated blast furnace slag, Mater. Des. 44 (2013) 500–508.
[35] K. Van Tittelboom, E. Gruyaert, H. Rahier, N. De Belie, Influence of mix composition on the extent of autogenous crack healing by continued hydration or calcium carbonate formation, Constr. Build. Mater. 37 (2012) 349–359.
[36] H. Huang, G. Ye, D. Damidot, Effect of blast furnace slag on self-healing of microcracks in cementitious materials, Cem. Concr. Res. 60 (2014) 68–82.
[37] M. Sahmaran, G. Yildirim, T.K. Erdem, Self-healing capability of cementitious composites incorporating different supplementary cementitious materials, Cem. Concr. Compos. 35 (1) (2012) 89–101.
[38] L.-L. Kan, H.-S. Shi, A.R. Sakulich, V.C. Li, Self-healing characterization of engineered cementitious composite materials, ACI Mater. J. 107 (6) (2010) 619–626.
[39] S. Fan, M. Li, X-ray computed microtomography of three-dimensional microcracks and self-healing in engineered cementitious composites, Smart Mater. Struct. 24 (1) (2014) 015021.
[40] H. Huang, G. Ye, D. Damidot, Characterization and quantification of self-healing behaviors of microcracks due to further hydration in cement paste, Cem. Concr. Res. 52 (2013) 71–81.
[41] S. Mindess, J.F. Young, D. Darwin, Concrete, 2003.
[42] B. Kolani, L. Buffo-Lacarrière, A. Sellier, G. Escadeillas, L. Boutillon, L. Linger, Hydration of slag-blended cements, Cem. Concr. Compos. 34 (9) (2012) 1009–1018.
[43] E.-H. Yang, S. Wang, Y. Yang, V.C. Li, Fiber-bridging constitutive law of engineered cementitious composites, J. Adv. Concr. Technol. 6 (1) (2008) 181–193.